Humidity sensor based on multi-layer graphene (MLG) integrated onto a micro-hotplate (MHP)

Sacco, Leandro Nicolas ; Meng, Hanxing ; Vollebregt, Sten

DOI
10.1109/SENSORS52175.2022.9967039

Publication date
2022

Document Version
Final published version

Published in
Proceedings of the 2022 IEEE Sensors

Humidity sensor based on multi-layer graphene (MLG) integrated onto a micro-hotplate (MHP)

Leandro Nicolas Sacco, Hanxing Meng, and Sten Vollebregt

Department of Microelectronics, Delft University of Technology, Feldmannweg 17, 2628 CT Delft, The Netherlands

l.n.sacco@tudelft.nl

0000-0002-5384-2020

***Abstract*—This work demonstrates a humidity sensor based on two multi-layered graphene (MLG) strips monolithically integrated onto a micro-hotplate (MHP). A transfer-free approach was adopted to release the graphene from the catalyst to reduce device variations and ensure scalability. The sensing performance of the device was tested by exposing the device to humidity levels in the range of 10% to 84% of relative humidity (RH). Both MLG strips present a linear response over this range. The micro-heater implementation is vital to fully desorb water molecules from the MLG surface. The micro-heater was powered with 31 mW to reach 140 °C in the MHP zone. The sensitivity of the devices is of the order of 1000 pp/RH[%]. The developed device aims at providing a robust and reliable gas sensors platform based on MLG.**

Keywords—Multi-layer graphene, microheater, humidity sensing, transfer-free graphene, gas sensors.

I. INTRODUCTION

Graphene-based gas sensors have attracted great interest in the scientific community due to their high sensitivity, chemical stability, and capability to introduce surface modifications for enhanced selectivity [1]. Particularly, for gas sensing applications the possibility of cross-sensitivity of humidity with target gas analytes can dramatically affect a device sensing performance [2], [3]. The integration of a micro-heater on the device sensors arises as an attractive solution to avoid the water molecules adsorption in the graphene sensing layer and/or improve the sensitivity of the sensing layer to a specific gas [4], [5]. Furthermore, at room temperature conditions, the activation energy is generally not sufficient for the desorption of gas and/or water molecules from the graphene surface which can conduct sluggish recoveries [6], [7]. Consequently, under optimal operational conditions, the micro-heater can serve to improve device sensitivity, desorb the undesirable water molecules of the sensing layer, and recover the device to the initial state. For this, graphene has to be integrated with a micro-heater which can be a challenge when transfer techniques are used.

Herein, we introduced a procedure to fabricate via a transfer-free method [8], multi-layered graphene (MLG)-based devices monolithically integrated on top of a micro-hot plate (MHP). The MLG was grown by a CVD process using Molybdenum (Mo) as a catalyst. Subsequently, the MLG was released using wet chemical etching. The adopted approach aims to avoid reproducibility issues relate to graphene transfer methods, e.g. due to polymer residues or damage to the graphene during transfer.

To demonstrate the working of the fabricated device as a potential gas sensor, humidity tests were performed. The fabricated devices provide an excellent platform to study the interaction of the MLG strips with water molecules, to eventually reduce the humidity cross-sensitivity for further gas sensing applications, and to effectively recover the device to an initial/reference resistivity value. From the presented results it is evident that the fabricated transfer-free MLG devices integrated onto a micro-heater are suitable for gas sensing applications.

II. EXPERIMENTAL SECTION

A. Device fabrication

The fabrication process of the MLG strips monolithically integrated into a micro-heater is shown in Fig. 1. A single-sided polished 525 µm thick 100 mm p-type <100> silicon wafer was used as substrate. First, the Si wafer was covered by a 500 nm-thick film of thermally grown SiO_2, followed by a low-stress 500 nm LPCVD SiNx deposition (Fig. 1.a). For the micro-heater design, a 200 nm thick Mo metal layer was sputtered on the front side of the wafer, followed by 350 nm-thick SiO_2 deposited by PECVD. Then the sacrificial SiO_2 hard mask was patterned, followed by a Mo etching step by a plasma etching process (Fig. 1.b). The patterned 350 nm-thick SiO_2 deposited by PECVD was removed in a buffered 1:7 HF etch solution, subsequently, another 350 nm-thick PECVD SiO_2 layer was deposited, followed by 250 nm low-stress LPCVD SiNx (Fig. 1.c). This stacking of SiO_2/SiNx works as an isolation layer that electrically insulates the Mo heaters electrodes and the future sensing layer. On the backside of the wafer, a 6 µm thick PECVD silicon SiO_2 was deposited, then, the patterned PECVD silicon SiO_2 was etched and subsequently, the SiNx layer was etched, both using fluorine plasma (Fig. 1.d). On the front side of the wafer, a 50 nm-thick Mo catalyst for the MLG synthesis was sputtered and patterned by plasma etching, then, the electrodes-pads from the heater were partially opened by plasma etching of the SiNx. The MLG synthesis was selectively performed on Mo using a commercially available AIXTRON BlackMagic Pro at 935°C using $Ar/H_2/CH_4$ as feedstock (Fig. 1.e). The micro-heaters pads were fully opened after 350 nm-thick SiO_2 by wet etching (Fig. 1.f). Subsequently, a negative resist lift-off process was carried out to make the four-probes electrical contacts on both, MLG and the micro-heater, by

2022 IEEE Sensors | 978-1-6654-8464-0/22/$31.00 ©2022 IEEE | DOI: 10.1109/SENSORS52175.2022.9967039

evaporating Cr/Au (10/100 nm) (Fig. 1.g). To finalize, the remaining SiO_2 layer on the backside was wet etched . Then, the Si etching from the backside was executed using a Bosch process. Afterwards, the devices were diced, Mo was etched using a transfer-free approach [8] (Fig.1.h) and wired bonded on ceramic PCB purchased at CERcircuits.

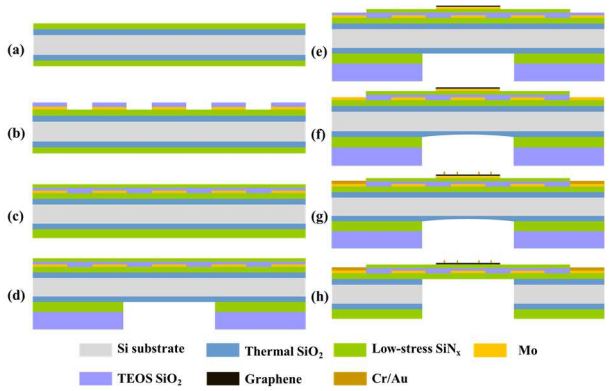

Fig. 1. The fabrication process of MLG strips integrated on a MHP. (a) Coating of the starting material with SiO_2/SiNx stacking. (b) Mo heater patterning. (c) Isolation layer of the Mo heater electrodes and the sensing layer. (d) Hard mask pattering on the backside for the Si cavity under the MHP. (e) Partially open pads step prior to the MLG synthesis. (f) Fully opened micro-heaters pad after SiO_2 removal. (g) Cr/Au electrodes evaporation. (h) MLG on the MHP after backside SiO2/Si etching and Mo catalyst etching.

B. Materials characterization

To determine the MHP temperature characteristics an infra-red thermal imaging camera VarioCam was used. Fig. 2 shows an optical image of the 2 MLG strips on the MHP (Fig. 2.a) and the thermal image when the heater was biased with 1.5 V (Fig. 2.b). The micro-heater power consumption was around 31 mW to reach an average temperature on the MHP of 140°C. The MHP diameter is 1 mm, then, the ratio of power per heated area is a good indicator of the micro-heater performance to make a better comparison with other MHP [9]. Herein, the power consumed per heated area is around $4x10^{-5}$ mW/µm^2. The patterned MLG strips are 200 µm x 20 µm.

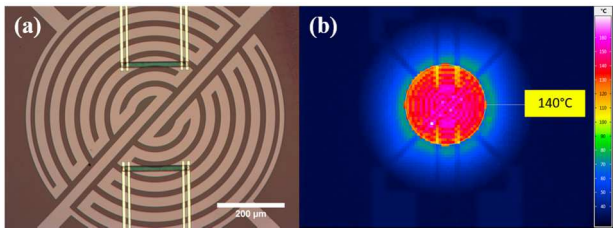

Fig. 2. (a) Optical image of the 2 MLG strips on the MHP. (b) Thermal image mapping of the MHP powered at 31 mW, the indicated temperature refers to the average temperature measured on the MHP.

C. Humidity sensing measurements

The humidity sensing properties of MLG strips were measured by acquiring the variation of the sheet resistance upon controlled exposure to water molecules. The sensor was loaded into a stainless steel chamber, where the transport properties of MLG and the micro-heater were measured as a function of time using a four-probe configuration with a Keithley 2612B source-meter-unit. One channel was devoted to the MLG strips and the remaining channel was used to control the micro-heater. A multiplexor Agilent 34970A data acquisition/switch unit was used to permute the resistance measurements between the two MLG strips. A labview script was developed to pilot the sensors and the MHP. The MLG devices were biased with 1V and the micro-heater with 1.5V when turned on.

The device response was defined as $R[\%]= 100\%\cdot(R_{Humid} - R_{Dry})/R_{Dry}$. Where R_{Humid} and R_{Dry} are sheet resistance measured during the exposure to water molecules during a humidity step and during the dry N_2 exposure, respectively. To desorb any impurity or water molecules already adsorbed in the device, and establish a reference value for the sheet resistance value, the sensor was purged with dry nitrogen (N_2) gas for 1.5 hours with the micro-heater pulsing between room temperature and 140°C with a period of 2.5 seconds.

A humidity generator (OHG-4, Owlstone) was used to introduce different levels of humidity inside the chamber. As a carrier gas 99.999% N_2 was used, and the dew point was measured at the gas outlet of the humidity generator. The MLG strips were exposed to different humidity levels in the range of 10% to 84%. Each humidity step was kept for 10 minutes before starting recovery with N_2.

III. Results and Discussions

In a first attempt, the MLG strips were exposed to different humidity levels without using the micro-heater to characterise the device response and the recovery time of the device during the purge phase. Fig. 3 shows the MLG sheet resistance variation upon exposure to water molecules. Interestingly, the sheet resistance immediately increases for both devices after flowing a RH of 10%, with a response device of approximately of 3.5%. The resistance increase is attributed to the water molecules adsorption in topological defects like grain boundaries that lead to an increase in the conductive channel due to the donor property of water and the p-type conductivity of graphene. [10]. The presented results indicated that the fabricated devices are sensitive to water molecules exposure.

A previous report working with MLG synthesized at similar conditions [11] shows a low-humidity response of the MLG-based device. But in that case, the SiO_2 is the dielectric layer used to insulate the MLG from the Si wafer. In the present work, the dielectric layer is a low-stress SiNx film layer that is intrinsically hydrophobic [12], then we can hypothesise that water molecules can preferentially be absorbed on the MLG surface rather than on the dielectric layer. In contrast, the SiO_2 is typically hydrophilic, then the water molecules can be favourably absorbed on the oxide surface [13]. Further studies are required to verify the influence of the dielectric layer on the graphene sensing properties.

As observed in fig. 3, the recovery to the initial sheet resistance value after the purge phase is not complete. A

drift in the response in the resistance variation is detected until the RH 84% level. When the humidity levels are decreased from 84% up to 10%, with purges steps in between, the device sheet resistance value is stabilized around 1950 Ω/□. In this case, the device response during the RH decreasing regime is highly affected. For instance, the device response for D1, in the last humidity step (10% RH) is around 0.6%. Similar results were obtained for device D2. This may indicate that water molecules adsorbed on the MLG surface are not removed during the purge step.

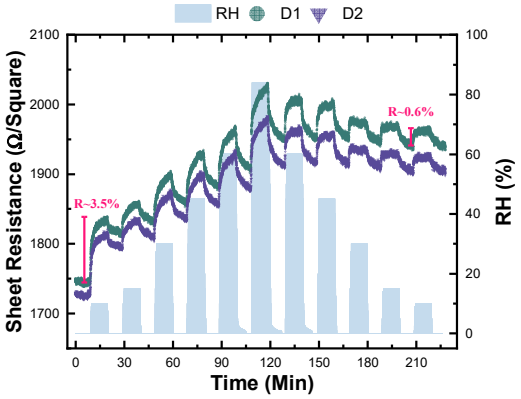

Fig. 3. MLG sheet resistance (left y-axis) of two devices based on MLG at different humidity steps (right y-axis). The two MLG strips devices are indicated by D1 and D2. The response at the first and last humidity steps is indicated in the plot.

Fig. 4 summarizes the device's performance when the identical humidity steps protocol was implemented, but now powering the micro-heater for 3 minutes after switching off the humidity at the end of each humidity step. As it is evident in Fig.4.a, the heating step efficiently promotes the water molecules desorption from the MLG devices after all humidity step exposure. The higher conductivity of the MLG devices when the MHP is powered is due to the negative thermal coefficient of resistance of MLG [14]. After an exposure of 84% of RH, the sheet resistance on both MLG devices during the heating step is stabilized already after 90 s, indicating that this time is enough to recover to the initial R_{Dry}.

The calibration curve is shown in Fig.4.b. The device responses were extracted at two intervals of the humidity exposure step. The responses were calculated doing an average of the sheet resistance value during the first (R-First Min) and last (R-Last Min) minute on each humidity step. For all cases, the slopes (i.e., the device sensitivity) vary from 1100-1480 ppm/ RH[%]. Better linearity of the calibration curve is obtained when the response value is obtained during the last minute of exposure, as is inferred from the R^2 values. Overall, both devices (D1 and D2) follow the same trend and the response in the decreasing humidity regime is barely changed, indicating a low hysteresis behaviour.

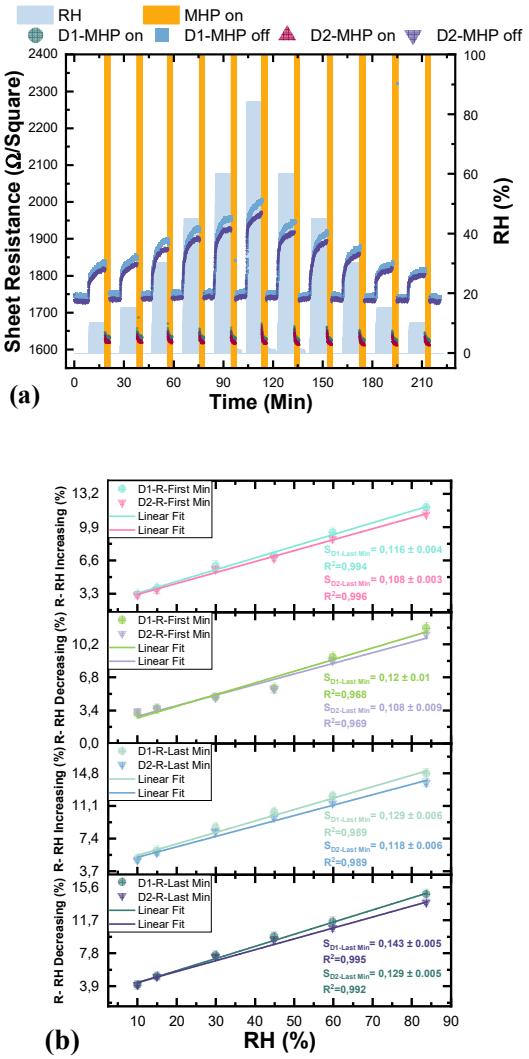

Fig. 4. (a) MLG sheet resistance (left y-axis) of two devices based on MLG at different humidity steps (right y-axis). The MHP was powered after each humidity step. The two MLG strip devices are indicated by D1 and D2. The responses at the first and last humidity steps are indicated in the plot. (b) Response as a function of the humidity level, where the response was calculated through the increasing and decreasing of the humidity steps during the first and last minute of H_2O exposure.

IV. Conclusions

This work introduces a procedure to fabricate a gas sensing-based MLG device using a transfer-free method, with an integrated micro-heater fully compatible with semiconductor fabrication. The device contains two MLG strips, each one connected by four electrodes. The device was tested as a humidity sensor, and globally the two MLG strips. The MLG has a linear behaviour in the range of 10-84% of RH with a sensitivity of the order of 1000 ppm/RH[%]. Further studies need to be performed to clarify the impact of the dielectric layer on the sensing mechanisms. The micro-heater is vital to obtain a device with linear response and to fully recover to the initial resistance. The MHP design can be further optimised to reduce the device's power consumption. The present work does not only aim to give tools to develop a humidity sensor but to also pave the way for the next generation of gas sensors based on MLG.

V. REFERENCING

[1] Z. Chen, J. Wang, and Y. Wang, "Strategies for the performance enhancement of graphene-based gas sensors: A review," *Talanta*, vol. 235, p. 122745, 2021, doi: https://doi.org/10.1016/j.talanta.2021.122745.

[2] H. Tang, L. N. Sacco, S. Vollebregt, H. Ye, X. Fan, and G. Zhang, "Recent advances in 2D/nanostructured metal sulfides-based gas sensors: mechanisms, applications, and perspectives," *J. Mater. Chem. A*, 2020, doi: 10.1039/D0TA08190F.

[3] S. Feng *et al.*, "Review on Smart Gas Sensing Technology," *Sensors* , vol. 19, no. 17. 2019, doi: 10.3390/s19173760.

[4] H. Ding *et al.*, "Recent Advances in Gas and Humidity Sensors Based on 3D Structured and Porous Graphene and Its Derivatives," *ACS Mater. Lett.*, vol. 2, no. 11, pp. 1381–1411, Nov. 2020, doi: 10.1021/acsmaterialslett.0c00355.

[5] Z. Yuan, F. Yang, and F. Meng, "Research Progress on Coating of Sensitive Materials for Micro-Hotplate Gas Sensor," *Micromachines* , vol. 13, no. 3. 2022, doi: 10.3390/mi13030491.

[6] J.-H. Kim, Q. Zhou, and J. Chang, "Suspended Graphene-Based Gas Sensor with 1-mW Energy Consumption," *Micromachines* , vol. 8, no. 2. 2017, doi: 10.3390/mi8020044.

[7] M. Lind *et al.*, "Semiquantitative Classification of Two Oxidizing Gases with Graphene-Based Gas Sensors," *Chemosensors* , vol. 10, no. 2. 2022, doi: 10.3390/chemosensors10020068.

[8] S. Vollebregt *et al.*, "A transfer-free wafer-scale CVD graphene fabrication process for MEMS/NEMS sensors," in *2016 IEEE 29th International Conference on Micro Electro Mechanical Systems (MEMS)*, 2016, pp. 17–20, doi: 10.1109/MEMSYS.2016.7421546.

[9] L. Mele *et al.*, "A molybdenum MEMS microhotplate for high-temperature operation," *Sensors Actuators A Phys.*, vol. 188, pp. 173–180, 2012, doi: https://doi.org/10.1016/j.sna.2011.11.023.

[10] V. I. Popov, D. V Nikolaev, V. B. Timofeev, S. A. Smagulova, and I. V Antonova, "Graphene-based humidity sensors: the origin of alternating resistance change," *Nanotechnology*, vol. 28, no. 35, p. 355501, 2017, doi: 10.1088/1361-6528/aa7b6e.

[11] F. Ricciardella, S. Vollebregt, T. Polichetti, P. M. Sarro, and G. S. Duesberg, "Low-Humidity Sensing Properties of Multi-Layered Graphene Grown by Chemical Vapor Deposition," *Sensors* , vol. 20, no. 11. 2020, doi: 10.3390/s20113174.

[12] A. Usenko and J. Senawiratne, "Silicon Nitride Surface Conversion into Oxide to Enable Hydrophilic Bonding," *ECS Trans.*, vol. 33, no. 4, pp. 475–483, 2010, doi: 10.1149/1.3483538.

[13] T. Arif, G. Colas, and T. Filleter, "Effect of Humidity and Water Intercalation on the Tribological Behavior of Graphene and Graphene Oxide," *ACS Appl. Mater. Interfaces*, vol. 10, no. 26, pp. 22537–22544, Jul. 2018, doi: 10.1021/acsami.8b03776.

[14] J. Romijn *et al.*, "Multi-layer graphene pirani pressure sensors," *Nanotechnology*, vol. 32, no. 33, p. 335501, 2021, doi: 10.1088/1361-6528/abff8e.